Constraining certain Higgs EFT couplings at the HL-LHC and beyond

Shankha Banerjee

IPPP, Durham University

April 17, 2018

Based on

Phys. Rev. D 89, 053010 (2014)

(with S. Mukhopadhyay and B.Mukhopadhyaya)

JHEP 1502 (2015) 128

(with G. Amar, S. Buddenbrock, A. Cornell, T.Mandal, B.Mellado and B. Mukhopadhyaya)

JHEP 1509 (2015) 057

(with T. Mandal, B. Mellado and B. Mukhopadhyaya)

ongoing work

(with R. S. Gupta, C. Englert and M. Spannowsky)

The story so far

- The nature of the discovered boson is more or less consistent with the *SM* Higgs
- Its combined (CMS + ATLAS) mass, from run-I data, is measured to be $M_h = 125.09 \pm 0.21$ (stat.) ± 0.11 (syst.) GeV in the $h \to \gamma\gamma$ and the $h \to ZZ^* \to 4\ell$ channels
- A *CP*-even spin zero hypothesis is favoured
- If it is "the Higgs", then its mass has fixed the *SM*
- Still to be measured: $h \to Z\gamma$, $h \to \mu^+\mu^-$, y_t, λ_{hhh}
- Till a reliable measurement of self-coupling is available it is best to consider the available final states that reflect the Higgs couplings

Signal strengths ($7 + 8$ TeV @ 25 fb^{-1})

Final states

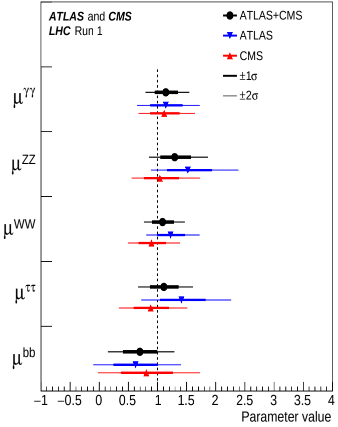

Production modes

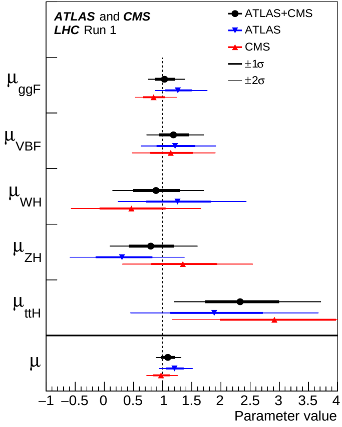

[arXiv:1606.02266]

Introduction

- Many reasons to go beyond the SM, *viz.* gauge hierarchy, neutrino mass, dark matter, baryon asymmetry etc.
- Plethora of BSM theories
- Two phenomenological approaches:
  - *Model dependent:* study the signatures of each model individually
  - *Model independent:* low energy effective theory formalism – analogous to Fermi's theory of beta decay
- The SM here is a low energy effective theory valid below a cut-off scale Λ
- A bigger theory is assumed to supersede the SM above the scale Λ
- At the perturbative level, all heavy ($> \Lambda$) DOF are decoupled from the low energy theory (Appelquist-Carazzone theorem)
- Appearance of HD operators in the effective Lagrangian valid below Λ

$$\mathcal{L} = \mathcal{L}_{SM}^{d=4} + \sum_{d\geq 5} \sum_{i} \frac{f_i}{\Lambda^{d-4}} \mathcal{O}_i^d$$

HD operators

- Higher-dimensional Operators: invariant under SM gauge group
- $d = 5$: Unique operator $\rightarrow$ Majorana mass to the neutrinos: $\frac{1}{\Lambda}(\Phi^\dagger L)^T C(\Phi^\dagger L)$
- $d = 6$: $59 = 15 + 19 + 25$ independent operators. Lowest dimension (after $d = 4$) which induces HVV interactions [W. Buchmuller and D. Wyler; B. Grzadkowski, M. Iskrzynski, M. Misiak and J. Rosiek; K.Hagiwara, D. Zeppenfeld et. al.]
- $d = 7$: Such operators appear in Higgs portal dark matter models
- $d = 8$: Lowest dimension inducing neutral TGC interactions
- To understand the EWSB sector better, we first consider a subset of $d = 6$ operators involving Φ, $\partial_\mu \Phi$, $X_{\mu\nu}$ (where $X = G, B, W$)

Gauge-invariant D6 CP$^+$ operators : Higgs-Gauge sector

- The operators containing the Higgs doublet Φ and its derivatives:

$$\mathcal{O}_{\Phi,1} = (D_\mu\Phi)^\dagger\Phi\Phi^\dagger(D^\mu\Phi); \quad \mathcal{O}_{\Phi,2} = \frac{1}{2}\partial_\mu(\Phi^\dagger\Phi)\partial^\mu(\Phi^\dagger\Phi); \quad \mathcal{O}_{\Phi,3} = \frac{1}{3}(\Phi^\dagger\Phi)^3$$

- The operators containing the Higgs doublet Φ (or its derivatives) and bosonic field strengths :

$$\mathcal{O}_{GG} = \Phi^\dagger\Phi G^a_{\mu\nu}G^{a\,\mu\nu}; \quad \mathcal{O}_{BW} = \Phi^\dagger\hat{B}_{\mu\nu}\hat{W}^{\mu\nu}\Phi; \quad \mathcal{O}_{WW} = \Phi^\dagger\hat{W}_{\mu\nu}\hat{W}^{\mu\nu}\Phi$$

$$\mathcal{O}_W = (D_\mu\Phi)^\dagger\hat{W}^{\mu\nu}(D_\nu\Phi); \quad \mathcal{O}_{BB} = \Phi^\dagger\hat{B}_{\mu\nu}\hat{B}^{\mu\nu}\Phi; \quad \mathcal{O}_B = (D_\mu\Phi)^\dagger\hat{B}^{\mu\nu}(D_\nu\Phi),$$

$\hat{W}^{\mu\nu} = i\,\frac{g}{2}\sigma_a W^{a\,\mu\nu}$, $\hat{B}^{\mu\nu} = i\,\frac{g}{2}'B^{\mu\nu}$; $\quad g$, g' : $SU(2)_L$, $U(1)_Y$ gauge couplings

$W^a_{\mu\nu} = \partial_\mu W^a_\nu - \partial_\nu W^a_\mu - g\epsilon^{abc}W^b_\mu W^c_\nu$; $\quad B_{\mu\nu} = \partial_\mu B_\nu - \partial_\nu B_\mu$

$G^a_{\mu\nu} = \partial_\mu G^a_\nu - \partial_\nu G^a_\mu - g_s f^{abc}G^b_\mu G^c_\nu$

Φ : Higgs doublet, $D_\mu\Phi = (\partial_\mu + \frac{i}{2}g'B_\mu + ig\frac{\sigma_a}{2}W^a_\mu)\Phi$: Covariant derivative

Properties of these operators

- $\mathcal{O}_{\Phi,1}$: Custodial symmetry violated $\rightarrow$ severely constrained by T-parameter
- $\mathcal{O}_{\Phi,2}$: Custodial symmetry preserved; modifies SM HVV couplings by multiplicative factors (same Lorentz structure)
- $\mathcal{O}_{\Phi,3}$: Modifies only the Higgs self-interaction; gives additional contribution to the Higgs potential
- $\mathcal{O}_{GG}$: Introduces HGG coupling with same Lorentz structure as in the SM; constrained from single Higgs production
- $\mathcal{O}_{BW}$: Drives tree-level $Z \leftrightarrow \gamma$ mixing $\rightarrow$ highly constrained by EWPT
- $\mathcal{O}_{WW}$, $\mathcal{O}_{W}$, $\mathcal{O}_{BB}$, $\mathcal{O}_{B}$: Modifies the HVV couplings by introducing new Lorentz structures in the Lagrangian; not all are severely constrained by the EWPT

Effective Lagrangian

$$\mathcal{L} = \beta \left(\frac{2m_W^2}{v} H W_\mu^+ W^{\mu -} + \frac{m_Z^2}{v} H Z_\mu Z^\mu \right) + \sum_i \frac{f_i}{\Lambda^2} \mathcal{O}_i$$

$$\begin{aligned} \mathcal{L}_{eff} \supset & g^{(1)}_{HWW} \left(W^+_{\mu\nu} W^{-\mu} \partial^\nu H + h.c. \right) + g^{(2)}_{HWW} \; H W^+_{\mu\nu} W^{-\mu\nu} \\ & + g^{(1)}_{HZZ} \; Z_{\mu\nu} Z^\mu \partial^\nu H + g^{(2)}_{HZZ} \; H Z_{\mu\nu} Z^{\mu\nu} \\ & + g^{(1)}_{HZ\gamma} \; A_{\mu\nu} Z^\mu \partial^\nu H + g^{(2)}_{HZ\gamma} \; H A_{\mu\nu} Z^{\mu\nu} + g_{H\gamma\gamma} H A_{\mu\nu} A^{\mu\nu}; \end{aligned}$$

$$g^{(1)}_{HWW} = \left(\frac{gM_W}{\Lambda^2} \right) \frac{f_W}{2}; \quad g^{(2)}_{HWW} = - \left(\frac{gM_W}{\Lambda^2} \right) f_{WW}$$

$$g^{(1)}_{HZZ} = \left(\frac{gM_W}{\Lambda^2} \right) \frac{c^2 f_W + s^2 f_B}{2c^2}; \quad g^{(2)}_{HZZ} = - \left(\frac{gM_W}{\Lambda^2} \right) \frac{s^4 f_{BB} + c^4 f_{WW}}{2c^2}$$

$$g^{(1)}_{HZ\gamma} = \left(\frac{gM_W}{\Lambda^2} \right) \frac{s(f_W - f_B)}{2c}; \quad g^{(2)}_{HZ\gamma} = \left(\frac{gM_W}{\Lambda^2} \right) \frac{s(s^2 f_{BB} - c^2 f_{WW})}{c}$$

$$g_{H\gamma\gamma} = - \left(\frac{gM_W}{\Lambda^2} \right) \frac{s^2 (f_{BB} + f_{WW})}{2}$$

Anomalous charged TGC interactions

We also consider the anomalous VVV interactions by

$$\mathcal{L}_{WWV} = -ig_{WWV}\{g_1^V\left(W^+_{\mu\nu}W^{-\mu}V^{\nu} - W^+_{\mu}V_{\nu}W^{-\mu\nu}\right) + \kappa_V W^+_{\mu}W^-_{\nu}V^{\mu\nu} + \frac{\lambda_V}{M_W^2}W^+_{\mu\nu}W^{-\nu\rho}V^{\mu}_{\rho}\}$$

where $g_{WWV} = g\, s$, $g_{WWZ} = g\, c$, $\kappa_V = 1 + \Delta\kappa_V$ and $g_1^Z = 1 + \Delta g_1^Z$ with

$$\Delta\kappa_\gamma = \frac{M_W^2}{2\Lambda^2}\left(f_W + f_B\right); \quad \lambda_\gamma = \lambda_Z = \frac{3g^2 M_W^2}{2\Lambda^2} f_{WWW}$$

$$\Delta g_1^Z = \frac{M_W^2}{2c^2\Lambda^2} f_W; \quad \Delta\kappa_Z = \frac{M_W^2}{2c^2\Lambda^2}\left(c^2 f_W - s^2 f_B\right)$$

Modified efficiencies: Case study ($pp \to Hjj \to WW^*jj$)

- We consider the $H \to WW^* + 2j$, $WW^* \to l^+\nu l^-\bar{\nu}$ ($l = \{e, \mu\}$) channel which includes contributions from both *VBF* and *VH* production modes.

$$\epsilon_{WW^*+\geq 2-\text{jets}} = \frac{50.98\beta^4 + 121.76\beta^3 f_{WW} + 22.85\beta^2 f_{WW}^2 + 0.15\beta f_{WW}^3 + 0.01 f_{WW}^4}{1601.43\beta^4 + 3796.63\beta^3 f_{WW} + 666.79\beta^2 f_{WW}^2 - 1.98\beta f_{WW}^3 + 0.73 f_{WW}^4}.$$

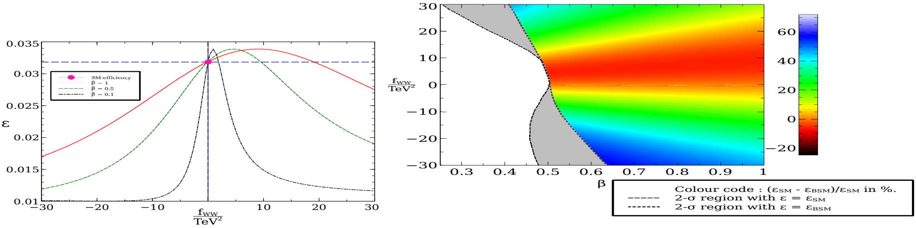

- Percentage modification of the combined efficiency of all cuts compared to the SM case. Grey region : $\epsilon_{BSM} = \epsilon_{SM}$

Phenomenology at e^+e^- colliders

Two main Higgs production processes are

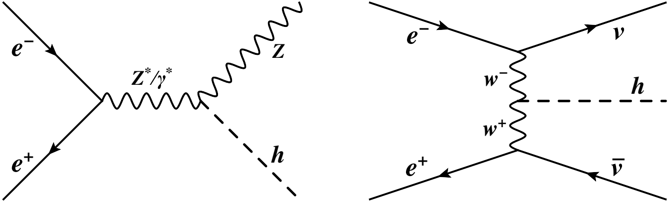

- $e^+e^- \to \nu\bar{\nu}H$ process $\to$ admixture of s and t-channel processes
- Possible to separate s and t-channel from $e^+e^- \to \nu\bar{\nu}H$ events by applying

$$E_H\text{-cut:} \quad \left| E_H - \frac{S + M_H^2 - M_Z^2}{2\sqrt{S}} \right| \leq \Delta (= 5 \text{ GeV})$$

- $\Delta \sim \Delta E_{jet}$ where $\Delta E_{jet}/E_{jet} \lesssim 0.3/\sqrt{E_{jet}}$. For two b-jets each with energy $\sim$100 GeV,$\Delta E_{jet} = \sqrt{2 \times (0.3 \times \sqrt{100})^2} \sim 4$ GeV

The amplitudes : An example

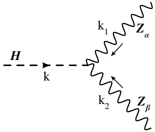

$$M = i(\frac{gM_W}{c})[\beta g^{\alpha\beta} + T^{\alpha\beta}]$$

$$T^{\alpha\beta} = \frac{1}{2\Lambda^2 c}\{4(s^4 f_{BB} + c^4 f_{WW})[g^{\alpha\beta}(k_1 \cdot k_2) - k_2^\alpha k_1^\beta] + (c^2 f_W + s^2 f_B)$$
$$\times[-g^{\alpha\beta}(k_1^2 + k_2^2 + 2k_1 \cdot k_2) + (k_1^\alpha k_1^\beta + 2k_2^\alpha k_1^\beta + k_2^\alpha k_2^\beta)]\}$$

- $\mathcal{M}_{e^+e^- \to ZH}$ is a linear combination of $x_i \in \{\beta, f_{WW}, f_W, f_{BB}, f_B\}$
- Cross-section can always be expressed as a bilinear combination

$$\sigma_{ZH}(\sqrt{S}, x_i) = \sum_{i,j=1}^{5} x_i C_{ij}(\sqrt{S}) x_j$$

Fitted cross-sections

$$\sigma(\sqrt{S}) = \mathcal{X} \cdot \mathcal{M}(\sqrt{S}) \cdot \mathcal{X}^T$$

where $\mathcal{X} = (\beta, f_{WW}, f_W, f_{BB}, f_B)$ is a row vector on parameter-space

$$\mathcal{M}^s_{ZH}(300\ GeV) = \begin{pmatrix} 181.67 & -6.43 & -2.99 & -0.51 & -0.71 \\ -6.43 & 0.46 & 0.18 & -0.03 & -0.08 \\ -2.99 & 0.18 & 0.14 & -0.02 & -0.06 \\ -0.51 & -0.03 & -0.02 & 0.02 & 0.03 \\ -0.71 & -0.08 & -0.06 & 0.03 & 0.08 \end{pmatrix}$$

$$\mathcal{M}^t_{\nu\bar{\nu}H}(300\ GeV) = \begin{pmatrix} 15.36 & 0.04 & 0.07 \\ 0.04 & 1.2 \times 10^{-3} & -7.7 \times 10^{-4} \\ 0.07 & -7.7 \times 10^{-4} & 4.6 \times 10^{-4} \end{pmatrix}$$

- σ^s is less sensitive on $\mathcal{O}_{BB}$ and $\mathcal{O}_B$ but σ^t is almost insensitive to HDOs

σ versus $\sqrt{S}$

Benchmark points: $BP1 = \{1, 0, 5, 0, 0\}$, $BP2 = \{1, 0, -5, 0, 0\}$ (allowed by $EWPT$ constraints and LHC data)

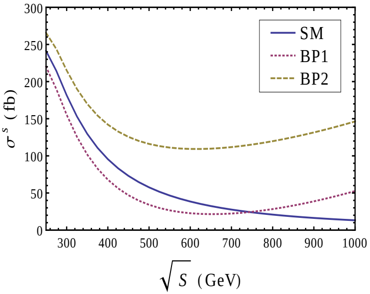

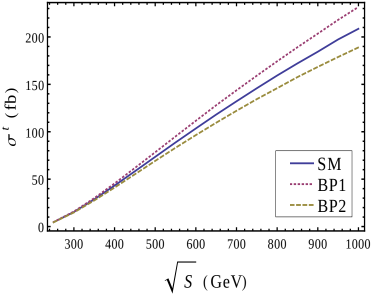

- In the SM: $\sigma_{ZH} \sim 1/S$ and $\sigma^t_{\nu\bar{\nu}H} \sim \ln(S/M_H^2)$
- In presence of HDOs, the $\sqrt{S}$-dependency is non-trivial especially for the s-channel process

θ_H distributions

Benchmark points: $BP3 = \{1, -3, 8, -4, 3\}$ (allowed by *EWPT* constraints and *LHC* data)

s-channel

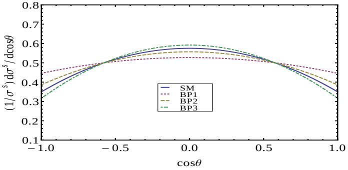

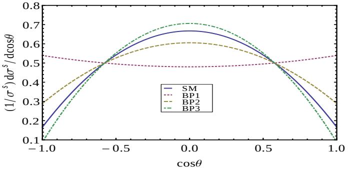

t-channel

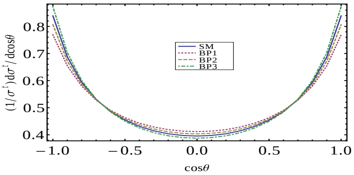

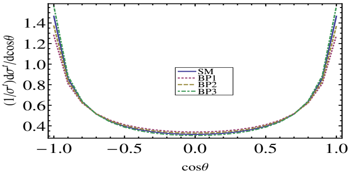

Top (bottom): $\sqrt{S} = 300\ (500)$ GeV

Varying two parameters at the same time

Two parameters are varied keeping others fixed ($\sqrt{S} = 300$ GeV). Brown patches signify $\sigma_{SM} \pm \sigma_{SM} \times 10\%$

s-channel

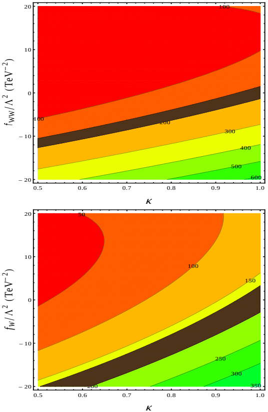

s-channel

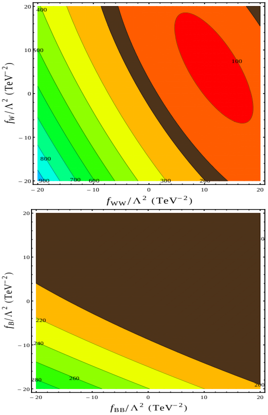

t-channel

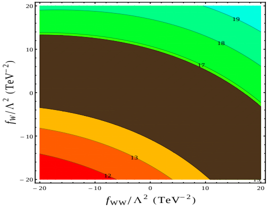

Estimating D6 coefficients at the HL-LHC

- The HD operator coefficients are constrained to values of $\mathcal{O}(1)/\text{TeV}^2$
- Kinematic variables can show very little variations *w.r.t.* the *SM* for such small coefficients
- One may construct observables sensitive to even small values of the operator coefficients
- Cross-sections and decay widths are sensitive observables
- If we construct ratios, many correlated uncertainties get cancelled

The ratio $\mathcal{R}_1$

$$\mathcal{R}_1(f_i) = \frac{\sigma_{\rm ggF} \times {\rm BR}_{H\to\gamma\gamma}(f_i)}{\sigma_{\rm ggF} \times {\rm BR}_{H\to WW^*\to 2\ell 2\nu}(f_i)}$$

$$\mathcal{R}_1(f_i) = \frac{\mu^{\rm ggF}_{\gamma\gamma}(f_i)}{\mu^{\rm ggF}_{WW^*}(f_i)} \times \frac{(\sigma_{\rm ggF} \times {\rm BR}_{H\to\gamma\gamma})^{\rm SM}}{(\sigma_{\rm ggF} \times {\rm BR}_{H\to WW^*\to 2\ell 2\nu})^{\rm SM}}$$

- Strong bounds on $\mathcal{O}_{WW}$ and $\mathcal{O}_{BB}$; insensitive to the other two operators $\mathcal{O}_W$ and $\mathcal{O}_B$
- $f_{WW} \approx f_{BB}$ allowed region $\approx [-2.76, -2.65] \cup [-0.06, 0.04]$ TeV^{-2}

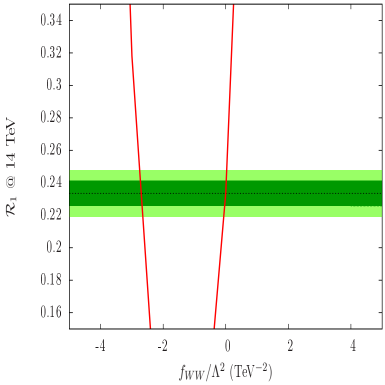

Figure : $\mathcal{R}_1$ versus f_{WW}/Λ^2 (TeV^{-2}). Red line → theoretical expectation in presence of HDOs; Dark green band → uncorrelated theoretical uncertainty; Light green band → total uncorrelated uncertainty at 14 TeV with 3000 fb^{-1} integrated luminosity; Black dotted line → central value.

The ratio $\mathcal{R}_2$

$$\mathcal{R}_2(f_i) = \frac{\sigma_{\rm VBF}(f_i) \times {\rm BR}_{H\to\gamma\gamma}(f_i)}{\sigma_{\rm WH}(f_i) \times {\rm BR}_{H\to\gamma\gamma}(f_i) \times {\rm BR}_{W\cdot}}$$

- We consider the bounds from $\mathcal{R}_1$ for $\mathcal{O}_{WW}$ and see that even such small values can be probed at 14 TeV $HL-LHC$
- f_{WW}/Λ^2 excluded region : $[-1.96, +1.62]$ TeV^{-2}, f_W/Λ^2 excluded region : $[-2.10, +2.50]$ TeV^{-2}

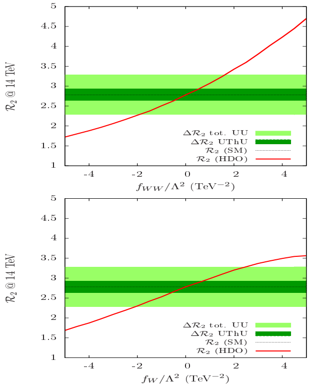

The ratio $\mathcal{R}_3$

$$\mathcal{R}_3(f_i) = \frac{\sigma_{\rm ggF} \times {\rm BR}_{H\to Z\gamma\to 2\ell\gamma}(f_i)}{\sigma_{\rm ggF} \times {\rm BR}_{H\to WW^*\to 2\ell 2\nu}(f_i)}$$

- $\mathcal{O}_B$ sensitive only to the ZZ^* and $Z\gamma$ channels.
- Sensitivity to ZZ^* is negligible. Sensitivity to $Z\gamma$ is strong, but $H \to Z\gamma$ is not yet measured.
- Projected bounds f_B/Λ^2 is $[-8.44, -7.17] \cup [-0.72, +0.56]$ TeV^{-2}.

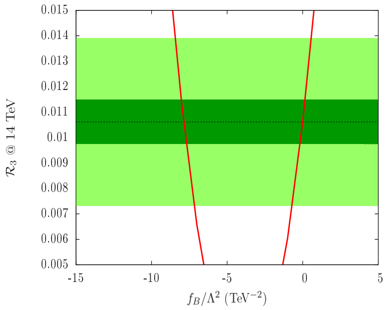

Constraining TGC couplings with $pp \to ZH$ at the HL-LHC

- We have seen from LEP that measuring the oblique S, T parameters can constrain several BSM scenarios at much higher scales than the LEP running energy
- Many vertices ensuing from EFT operators are correlated and hence LEP has already constrained certain operators affecting the Higgs vertices
- We target the higher energy regions in the parameter space in order to compete with the LEP constraints [See Rick's slides for more details]

Constraining TGC couplings with $pp \to ZH$ at the HL-LHC

$$
\begin{aligned}
\Delta\mathcal{L}_6 \;\supset\; & \sum_f \delta g_f^Z Z_\mu \bar{f}\gamma^\mu f + \delta g_{ud}^W (W_\mu^+ \bar{u}_L \gamma^\mu d_L + h.c.) \\
+\; & g_{VV}^h\, h \left[W^{+\mu} W_\mu^- + \frac{1}{2c_{\theta_W}^2} Z^\mu Z_\mu \right] + \delta g_{ZZ}^h\, h \frac{Z^\mu Z_\mu}{2c_{\theta_W}^2} \\
+\; & \sum_f g_{Zff}^h \frac{h}{v} Z_\mu \bar{f}\gamma^\mu f + g_{Wud}^h \frac{h}{v} (W_\mu^+ \bar{u}_L \gamma^\mu d_L + h.c.) \\
+\; & \kappa_{Z\gamma} \frac{h}{v} A^{\mu\nu} Z_{\mu\nu} + \kappa_{WW} \frac{h}{v} W^{+\mu\nu} W_{\mu\nu}^- + \kappa_{ZZ} \frac{h}{2v} Z^{\mu\nu} Z_{\mu\nu}
\end{aligned}
$$

The $qq \to Vh$ amplitude can be expressed as

$$
\mathcal{M}(ff \to Vh) = \frac{1}{v} \epsilon^{*\mu}(q)\, J_f^{V\,\nu}(p) \left[A_f^V \eta_{\mu\nu} + B_f^V \,(p\cdot q\, \eta_{\mu\nu} - p_\mu q_\nu) \right] \qquad J_f^\mu = \bar{f}\gamma^\mu f
$$

$$
A_f^V = a_f^V + \widehat{a}_f^V \frac{m_V^2}{p^2 - m_V^2} \qquad B_f^V = b_f^V \frac{1}{p^2 - m_V^2} + \widehat{b}_f^V \frac{1}{p^2}
$$

$$
\begin{aligned}
a_f^Z &= g_{Zff}^h & a_f^W &= g_{Wff'}^h\,, \\
\hat{a}_f^Z &= 2g_f^Z + \frac{g_f^Z v}{m_W^2} \left(\delta g_{VV}^h + v\delta g_{ZZ}^h \right)\,, & \hat{a}_f^W &= 2g_f^W + \frac{\delta g_{VV}^h g_f^W v}{m_W^2}\,, \\
b_f^Z &= -4 g_f^Z \kappa_{ZZ}\,, & b_f^W &= -2 g_f^W \kappa_{WW}\,, \\
b_f^Z &= -2eQ_f t_{\theta_W} \kappa_{Z\gamma}\,,
\end{aligned}
$$

$$
g_f^Z = \frac{g}{c_{\theta_W}} (T_3 - Q_f s_{\theta_W}^2) \qquad g_f^W = \frac{g}{\sqrt{2}}.
$$

Constraining TGC couplings with $pp \to ZH$ at the HL-LHC

$$
\begin{aligned}
\Delta\mathcal{L}_6 \supset & \sum_f \delta g_f^Z Z_\mu \bar{f}\gamma^\mu f + \delta g_{ud}^W (W_\mu^+ \bar{u}_L \gamma^\mu d_L + h.c.) \\
+ & \; g_{VV}^h h \left[W^{+\mu}W_\mu^- + \frac{1}{2c_{\theta_W}^2} Z^\mu Z_\mu \right] + \delta g_{ZZ}^h h \frac{Z^\mu Z_\mu}{2c_{\theta_W}^2} \\
+ & \sum_f g_{Zff}^h \frac{h}{v} Z_\mu \bar{f}\gamma^\mu f + g_{Wud}^h \frac{h}{v} (W_\mu^+ \bar{u}_L \gamma^\mu d_L + h.c.)
\end{aligned}
$$

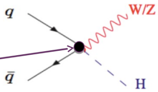

Leading effect from contact interaction at high energies.
Energy growth as there is no propagator.

$$
\mathcal{M}(ff \to Z_L h) = g_f^Z \frac{q \cdot J_f}{v} \frac{2m_Z}{\hat{s}} \left[1 + \frac{g_{Zff}^h}{g_f^Z} \frac{\hat{s}}{2m_Z^2} \right]
$$

At high energies, the following four directions in the EFT parameter space are isolated by ZH production

$$
\begin{aligned}
g_{Zu_Lu_L}^h &= -\frac{g}{c_{\theta_W}} \left((c_{\theta_W}^2 + \frac{s_{\theta_W}^2}{3})\delta g_1^Z + W - \frac{t_{\theta_W}^2}{3}(\hat{S} - \delta\kappa_\gamma - Y) \right) \\
g_{Zd_Ld_L}^h &= -\frac{g}{c_{\theta_W}} \left((c_{\theta_W}^2 - \frac{s_{\theta_W}^2}{3})\delta g_1^Z + W + \frac{t_{\theta_W}^2}{3}(\hat{S} - \delta\kappa_\gamma - Y) \right) \\
g_{Zu_Ru_R}^h &= \frac{4g s_{\theta_W}^2}{3c_{\theta_W}^3} (\hat{S} - \delta\kappa_\gamma + c_{\theta_W}^2 \delta g_1^Z - Y) \\
g_{Zd_Rd_R}^h &= -\frac{2g s_{\theta_W}^2}{3c_{\theta_W}^3} (\hat{S} - \delta\kappa_\gamma + c_{\theta_W}^2 \delta g_1^Z - Y)
\end{aligned}
$$

$pp \to ZH$ at high energies

- We study the impact of constraining TGC couplings at higher energies
- We study the channel $pp \to ZH \to \ell^+\ell^- b\bar{b}$
- The backgrounds are SM $pp \to ZH$, $Zb\bar{b}$, $t\bar{t}$ and the fake $pp \to Zjj$ ($j \to b$ fake rate taken as 2%)
- Major background $Zb\bar{b}$
- Boosted substructure analysis with fat-jets of $R = 1.5$ used

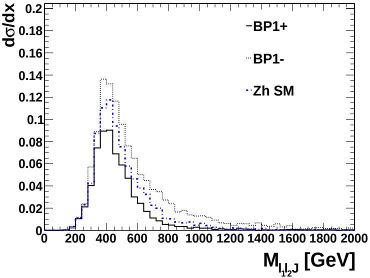

Cuts	Zbb	Zh
1. 2 B-mesons (with pT > 15 GeV) within R = 1.5	0.03	0.22
2. 2 isolated leptons (pT > 10 GeV) OSSF	0.48	0.53
3. 80 GeV < M_ll < 100 GeV, pT_ll > 100 GeV and DR(ll) > 0.2	0.61	0.83
3. >= 1 fat jet with 2 B-mesons and pT(jet) > 110 GeV	0.91	0.97
4. 2 Mass drop and >=2 filtered subjets	0.99	0.99
5. Double b-tag (70%, 2% mistag)	0.38	0.41
6. 115 GeV < M_bb < 135 GeV	0.19	0.40

$pp \to Zh$ at high energies

- Next we perform a two-parameter χ^2-fit (at 300 fb^{-1}) to find the allowed region in the $\delta g_1^Z - (\delta\kappa_\gamma - \hat{S})$

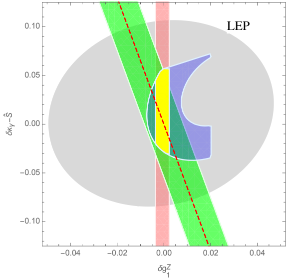

Grey region: LEP exclusion; pink band: exclusion from WZ [Franceschini, Panico, Pomarol, Riva and Wulzer, 2017];

Green (blue) region: exclusion from ZH with only interference (interference plus squared) term

Summary and conclusions

- EFT framework is a powerful tool to understand Higgs coupling deviations and nature of the Higgs (part of a doublet or not?)
- Efficiencies for various acceptance cuts are altered by varying Lorentz structure
- Future e^+e^- colliders can potentially constrain EFT parameters to excellent precision
- Various ratios can be used to see the effect of small values of operator coefficients $\rightarrow$ cancellation of several uncertainties
- Possible to constrain certain EFT parameters to stronger degrees at HL-LHC than was done at LEP
- Boosted ZH channel helps in constraining TGC couplings

Backup: Ranges of $\mathcal{R}_1, \mathcal{R}_2$ and $\mathcal{R}_3$

Observable	$\mathcal{O}_{WW}$	$\mathcal{O}_{BB}$	$\mathcal{O}_{W}$	$\mathcal{O}_{B}$
$\mathcal{R}_1$ @ 7+8 TeV	$[-3.32, -2.91] \cup [+0.12, +0.57]$	$[-3.32, -2.91] \cup [+0.12, +0.57]$	Not bounded	Not bounded
$\mathcal{R}_1$ @ 14 TeV	$[-2.76, -2.65] \cup [-0.06, +0.04]$	$[-2.76, -2.65] \cup [-0.06, +0.04]$	Not bounded	Not bounded
$\mathcal{R}_2$ @ 14 TeV	$[-1.96, +1.62]$	Not bounded	$[-2.10, +2.50]$	Not bounded
$\mathcal{R}_3$ @ 14 TeV	Not used	Not used	Not used	$[-8.44, -7.17] \cup [-0.72, +0.56]$

Backup

$$
\begin{aligned}
g^h_{Zu_Lu_L} &= -\frac{g}{c_{\theta_W}}\left((c^2_{\theta_W}+\frac{s^2_{\theta_W}}{3})\delta g^Z_1 + W - \frac{t^2_{\theta_W}}{3}(\hat{S}-\delta\kappa_\gamma - Y)\right)\\
g^h_{Zd_Ld_L} &= -\frac{g}{c_{\theta_W}}\left((c^2_{\theta_W}-\frac{s^2_{\theta_W}}{3})\delta g^Z_1 + W + \frac{t^2_{\theta_W}}{3}(\hat{S}-\delta\kappa_\gamma - Y)\right)\\
g^h_{Zu_Ru_R} &= \frac{4gs^2_{\theta_W}}{3c^3_{\theta_W}}(\hat{S}-\delta\kappa_\gamma + c^2_{\theta_W}\delta g^Z_1 - Y)\\
g^h_{Zd_Rd_R} &= -\frac{2gs^2_{\theta_W}}{3c^3_{\theta_W}}(\hat{S}-\delta\kappa_\gamma + c^2_{\theta_W}\delta g^Z_1 - Y)
\end{aligned}
$$

$$
\begin{aligned}
g^h_{Zu_Lu_L} &= -\frac{g}{c_{\theta_W}}\frac{m^2_W}{\Lambda^2}(c_W + c_{HW} - c_{2W} - \frac{t^2_{\theta_W}}{3}(c_B + c_{HB} - c_{2B}))\\
g^h_{Zd_Ld_L} &= -\frac{g}{c_{\theta_W}}\frac{m^2_W}{\Lambda^2}(c_W + c_{HW} - c_{2W} + \frac{t^2_{\theta_W}}{3}(c_B + c_{HB} - c_{2B}))\\
g^h_{Zu_Ru_R} &= \frac{4gs^2_{\theta_W}}{3c^3_{\theta_W}}\frac{m^2_W}{\Lambda^2}(c_B + c_{HB} - c_{2B})\\
g^h_{Zd_Rd_R} &= -\frac{2gs^2_{\theta_W}}{3c^3_{\theta_W}}\frac{m^2_W}{\Lambda^2}(c_B + c_{HB} - c_{2B})
\end{aligned}
$$